

In situ probing electrical response on bending of ZnO nanowires inside transmission electron microscope

K. H. Liu, P. Gao, Z. Xu, X. D. Bai, and E. G. Wang

Citation: *Appl. Phys. Lett.* **92**, 213105 (2008); doi: 10.1063/1.2936080

View online: <http://dx.doi.org/10.1063/1.2936080>

View Table of Contents: <http://aip.scitation.org/toc/apl/92/21>

Published by the [American Institute of Physics](#)



**THE WORLD'S RESOURCE FOR
VARIABLE TEMPERATURE
SOLID STATE CHARACTERIZATION**



OPTICAL STUDIES SYSTEMS



SEEBECK STUDIES SYSTEMS



MICROPROBE STATIONS



HALL EFFECT STUDY SYSTEMS AND MAGNETS



WWW.MMR-TECH.COM

In situ probing electrical response on bending of ZnO nanowires inside transmission electron microscope

K. H. Liu, P. Gao, Z. Xu, X. D. Bai,^{a)} and E. G. Wang

Beijing National Laboratory for Condensed Matter Physics and Institute of Physics, Chinese Academy of Sciences, Beijing 100080, People's Republic of China

(Received 3 January 2008; accepted 1 May 2008; published online 28 May 2008)

In situ electrical transport measurements on individual bent ZnO nanowires have been performed inside a high-resolution transmission electron microscope, where the crystal structures of ZnO nanowires were simultaneously imaged. A series of consecutively recorded current-voltage (*I-V*) curves along with an increase in nanowire bending show the striking effect of bending on their electrical behavior. The bending-induced changes of resistivity, electron concentration, and carrier mobility of ZnO nanowires have been retrieved based on the experimental *I-V* data, which suggests the applications of ZnO nanowires as nanoelectromechanical sensors. © 2008 American Institute of Physics. [DOI: 10.1063/1.2936080]

Nanoscale one-dimensional ZnO materials, such as nanowires¹ and nanobelts,² have attracted great interest due to their importance both in basic scientific research and in potential technological applications. As a prototype material, the mechanical properties of ZnO nanowires^{3–6} and ZnO nanobelts^{7,8} have been investigated. Recently, the nanogenerators,⁹ piezoelectric field effect transistors,¹⁰ and piezoelectric diodes¹¹ based on ZnO nanowires have been developed by the unique coupling of piezoelectric and semiconducting properties of ZnO, and then a new field nanopiezotronics has been set up.¹² For the piezorelated devices, electromechanical behavior plays a key role in their applications.

In this letter, we present electrical measurements of individual ZnO nanowires in combination with the determination of their crystal structure via *in situ* high-resolution transmission electron microscopy (TEM) technique. Thus, the electrical properties of ZnO nanowires were directly linked with their structure. In the meantime, the electrical response on the bending of ZnO nanowires was systematically investigated.

For *in situ* measuring the electrical transport properties of nanomaterials, a special specimen holder was designed in a JEOL 2010 field emission gun TEM, operated in a 10^{–5} Pa vacuum and at room temperature. This equipment has been used to study the mechanical properties of WO₃ nanowires¹³ and field emission properties of carbon nanotubes.^{14,15} ZnO nanowires were synthesized by the thermal evaporation of ZnO powders. To carry out electrical measurements *in situ* TEM, an individual ZnO nanowire was attached to the electrochemically etched tungsten tips by a dielectrophoresis method. The tungsten tips with ZnO nanowires were then loaded to the specimen holder and approached to its opposite gold electrode by a piezomanipulator. In order to achieve a good physical contact at the two ends of the ZnO nanowire, we first applied a relatively high voltage with a current of about 1 μA for 1 min. Because of the high resistance at the two contact points of the nanowire ends, a locally high temperature by the Joule heating could weld the nanowire onto

its two electrodes, so a perfect electrical contact and a tight fix were realized. While performing the electrical measurements, we blacked out the TEM electron beam to rule out the influence of electron bombardment.

Figures 1(a)–1(d) display the sequential images of a typical bending process of ZnO nanowires under the gentle moves of a piezodriven electrode. No slides at the two contact points between the nanowire and its electrodes were observed, showed by the inset arrowheads. Figures 1(e) and 1(f) are the *in situ* selected-area electron diffraction pattern and the high-resolution TEM image corresponding to the framed area in Fig. 1(a), which indicates that the ZnO nanowires have wurtzite structure and are high-quality single crystalline with the [01 $\bar{1}$ 0] growth direction. Figure 1(g) shows the consecutively recorded *I-V* curves along with an increase in nanowire bending process corresponding to the cases of Figs. 1(a)–1(d). For an initial two-end clamped not-bent ZnO nanowire, the highest conductance was demonstrated. With the increase in bending, the conductance dropped significantly, *vice versa*, the *I-V* characteristics was recovered with the decrease in the bending deformation.

The measured system in our experiment can be regarded as a metal-semiconductor-metal¹⁶ (*M-S-M*) circuit. Thus, the changes of electrical parameters can be retrieved from the experimental *I-V* data. The *I-V* curves are close to a straight line under the higher bias; their slopes are directly related to the resistances [$R=(dV/dI)$]. Based on the *M-S-M* model, under the lower bias, the current is expressed as^{17,18}

$$\ln I = \ln S + V \left(\frac{q}{k_B T} - \frac{1}{E_0} \right) + \ln J_S. \quad (1)$$

The $\ln I-V$ curves under lower bias are basically fitted to straight lines; their slope k is used to extract the carrier concentration n . The relationship between the slope k and n can be deduced by the following equations:

$$k = \frac{q}{k_B T} - \frac{1}{E_0}, \quad (2)$$

where $E_0 = E_{00} \coth(E_{00}/k_B T)$, $E_{00} = (\hbar q/2)(n/m^* \epsilon)^{1/2}$, q is the elemental charge, k_B is Boltzmann constant, m^* is an effective electron mass of the ZnO nanowire, and ϵ is the

^{a)} Author to whom correspondence should be addressed. Electronic mail: xdbai@aphy.iphy.ac.cn.

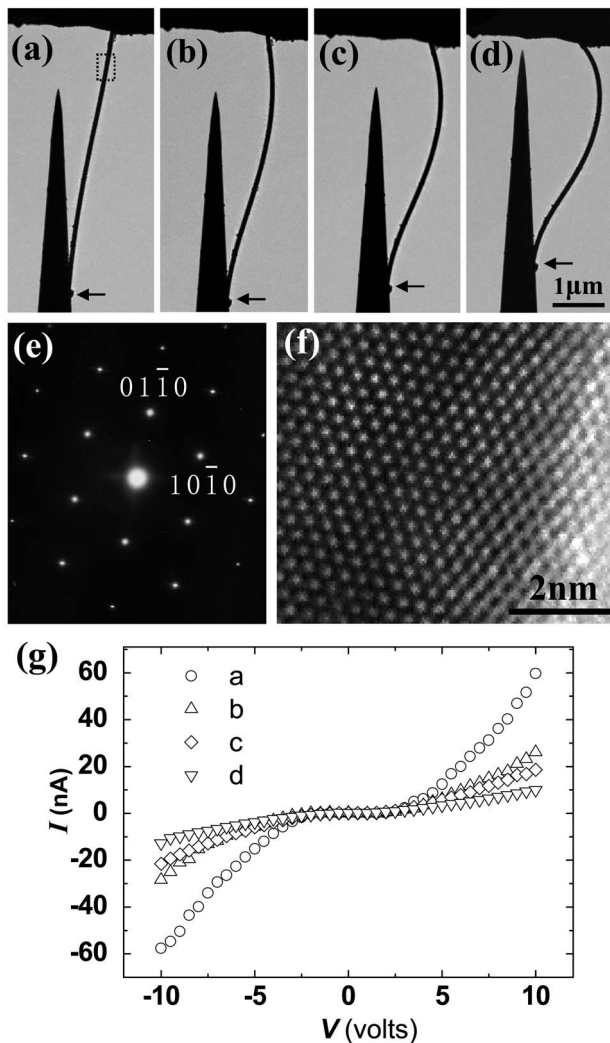


FIG. 1. [(a)–(d)] Sequential TEM images of the four typical bending cases of the ZnO nanowire. (e) Electron diffraction pattern of the framed area in (a), indicating that the nanowire has a wurtzite structure with the $[01\bar{1}0]$ growth direction. (f) The corresponding high-resolution TEM image of the framed area in (a), showing the high-quality single crystal. (g) A series of representative I - V curves of the ZnO nanowire, corresponding to the bending cases in (a)–(d).

dielectric constant. The specific sizes of nanowires are directly obtained inside TEM, so that the resistivity ρ can be obtained, and the electron mobility μ is then obtained by using the relationship $\mu = 1/(nq\rho)$.

The logarithmic plot of a current I as a function of a bias V gives an approximately straight line with a slope of k . A representative $\ln I$ - V curve is depicted in Fig. 2, corresponding to the curve c in Fig. 1(g). For ZnO materials, $\epsilon = 7.8\epsilon_0$, ϵ_0 is dielectric constant of vacuum and $m^* = 0.28m_0$.¹⁹ Thus, the electron concentration n can be acquired, and the electron mobility μ can then be obtained from the resistivity ρ of the nanowire. Applying this procedure to all the I - V curves in Fig. 1(g), the bent ZnO nanowire resistivity, electron concentration, and carrier mobility can be systematically extracted.

Herein, we simply use the proportion of the deflection of one nanowire end Δy_m to its length L ($\Delta y_m/L$) to describe the bending deformation of the ZnO nanowires, as shown schematically in Fig. 3(a). With the increase in bending, resistivity ρ , electron concentration n , and electron mobility μ of the ZnO nanowire obviously changed. The results are

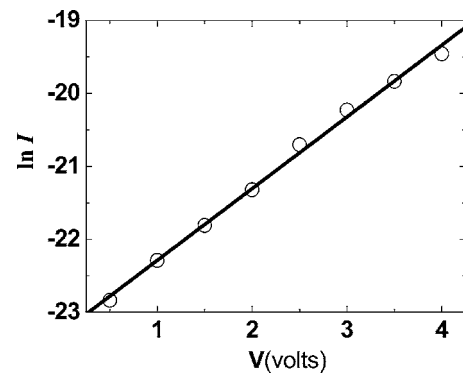


FIG. 2. A typical $\ln I$ - V curve of the ZnO nanowire at lower bias, corresponding to the curve c in Fig. 1(g).

summarized in Figs. 3(b)–3(d). The resistivity ρ increases considerably with increase in bending deformation $\Delta y_m/L$ [Fig. 3(b)]; the ρ - $\Delta y_m/L$ curve can be basically fitted to a straight line at a moderate deformation. The sensitivity of ρ to the mechanical deformation $\Delta y_m/L$ is estimated as $s = d\rho/d(\Delta y_m/L) = 120 \Omega \text{ cm}$, which implies that the ZnO nanowires could be applied as nanoelectromechanical sensors.

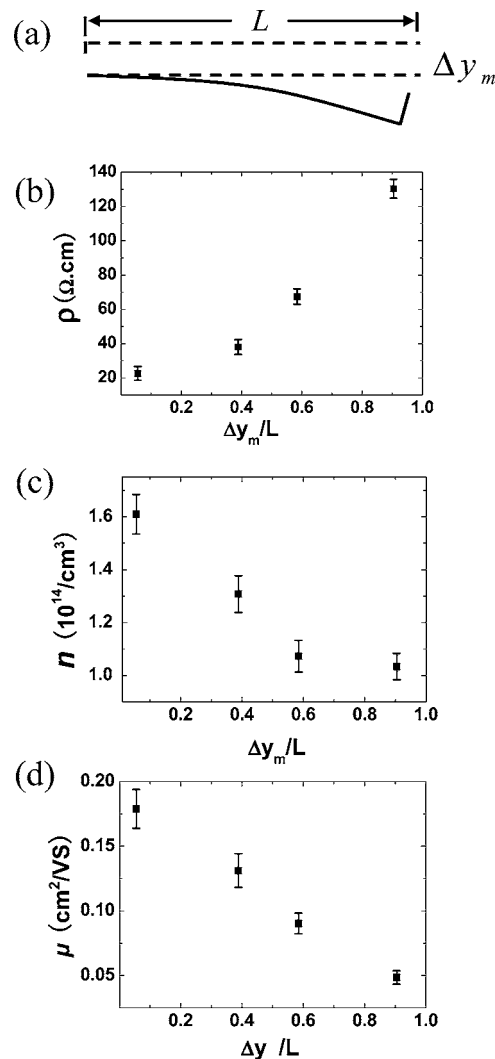


FIG. 3. (a) Simplified scheme of the deflected ZnO nanowires. [(b)–(d)] The dependence of resistivity ρ , electron concentration n , and carrier mobility μ on the nanowire bending deflection $\Delta y_m/L$.

From the fundamental knowledge, the change of ρ attributes to the change of n and μ . While $\Delta y_m/L$ increased, both n and μ decreased, and n had a tendency of saturation when $\Delta y_m/L$ exceeded 0.6 [Fig. 3(c)]. As proposed by Wang *et al.*,¹⁰ the electrical response on the bending of ZnO nanowires could be understood based on the piezoelectric effect of ZnO. In this study, the growth direction of ZnO nanowires is $[01\bar{1}0]$, as detected by *in situ* TEM [Figs. 1(e) and 1(f)], the polarization planes are parallel along with the nanowire length. A bent ZnO nanowire can produce a positively charged and negatively charged surface at the outer and inner bending arc surfaces of the nanowire due to the stretching and compression on the surface, respectively. The charges are static and nonmobile ionic charges, which induce a local electric field across the width of the nanowire. Under the local electric field, electrons are trapped on the positive charge side and become nonmovable charges, so the electron concentration n decreases as the nanowire bends, which is in consistence with the experimental results [Fig. 3(c)]. When the nanowire is bent to a critical degree, the electron trapping region is limited because the size of the conduction channel cannot be reduced again. Thus, the electron concentration n displays a tendency of saturation when $\Delta y_m/L$ exceeds 0.6. In addition, these polarized charges on the strain-free plane will influence the mobility μ , which may be contributed to the Coulomb charge scattering effect.^{20,21} It is shown that μ decreases monotonically with the gathering of polarized charges, which is crucial for the validity of the ZnO nanowire as a mechanical sensor even in the large bending deformation.

In summary, we present *in situ* manipulation and electrical transport measurements on individual ZnO nanowires inside a high-resolution TEM, where the crystal structures of ZnO nanowires were simultaneously imaged. Such that the electrical behaviors of ZnO nanowires were directly linked with their structure. With increasing the bending of ZnO nanowires, their conductance dropped significantly. The changes in electrical parameters, such as resistivity, electron concentration, and carrier mobility, have been retrieved

based on the experimental *I-V* curves, which suggests that ZnO nanowires have a promising application as nanoelectromechanical sensors.

The authors are grateful for the financial support of the NSF (Grant Nos. 50725209 and 60621091), the MOST (Grant No. 2007CB936203), and the CAS (Grant Nos. KJCX2-YW-M04 and GJHZ0611) of China. We also thank Professor Z. L. Wang at Georgia Tech. for his helpful discussions.

- ¹M. H. Huang, S. Mao, H. Feick, H. Yan, Y. Wu, K. Kind, E. Weber, R. Russo, and P. Yang, *Science* **292**, 1897 (2001).
- ²Z. W. Pan, Z. R. Dai, and Z. L. Wang, *Science* **291**, 1974 (2001).
- ³C. Q. Chen, Y. Shi, Y. S. Zhang, J. Zhu, and Y. J. Yan, *Phys. Rev. Lett.* **96**, 075505 (2006).
- ⁴J. Song, X. Wang, E. Riedo, and Z. L. Wang, *Nano Lett.* **5**, 1954 (2005).
- ⁵C. Q. Chen and J. Zhu, *Appl. Phys. Lett.* **90**, 043105 (2007).
- ⁶Y. Shi, C. Q. Chen, Y. S. Zhang, J. Zhu, and Y. J. Yan, *Nanotechnology* **18**, 075709 (2007).
- ⁷K. Yum, Z. Wang, A. P. Suryavanshi, and M. F. Yu, *J. Appl. Phys.* **96**, 3933 (2004).
- ⁸W. J. Mai and Z. L. Wang, *Appl. Phys. Lett.* **89**, 073112 (2006).
- ⁹Z. L. Wang and J. H. Song, *Science* **312**, 242 (2006).
- ¹⁰X. D. Wang, J. Zhou, J. H. Song, J. Liu, N. S. Xu, and Z. L. Wang, *Nano Lett.* **6**, 2768 (2006).
- ¹¹J. H. He, C. L. Hsin, J. Liu, L. J. Chen, and Z. L. Wang, *Adv. Mater. (Weinheim, Ger.)* **19**, 781 (2007).
- ¹²Z. L. Wang, *Adv. Mater. (Weinheim, Ger.)* **19**, 889 (2007).
- ¹³K. H. Liu, W. L. Wang, Z. Xu, L. Liao, X. D. Bai, and E. G. Wang, *Appl. Phys. Lett.* **89**, 221908 (2006).
- ¹⁴Z. Xu, X. D. Bai, E. G. Wang, and Z. L. Wang, *Appl. Phys. Lett.* **87**, 163106 (2005).
- ¹⁵Z. Xu, X. D. Bai, and E. G. Wang, *Appl. Phys. Lett.* **88**, 133107 (2006).
- ¹⁶F. A. Padovani and R. Stratton, *Solid-State Electron.* **9**, 695 (1966).
- ¹⁷Z. Y. Zhang, C. H. Jin, X. L. Liang, Q. Chen, and L. M. Peng, *Appl. Phys. Lett.* **88**, 73102 (2006).
- ¹⁸X. D. Bai, D. Golberg, Y. Bando, C. Y. Zhi, C. C. Tang, M. Mitome, and K. Kurashima, *Nano Lett.* **7**, 632 (2007).
- ¹⁹J. Hinze and K. Ellmer, *J. Appl. Phys.* **88**, 244 (2000).
- ²⁰H. M. Ng, D. Doppalapudi, T. D. Moustakas, N. G. Weimann, and L. F. Eastman, *Appl. Phys. Lett.* **73**, 821 (1998).
- ²¹Y. Furukawa, H. Yonezu, A. Wakahara, Y. Yoshizumi, Y. Morita, and A. Sato, *Appl. Phys. Lett.* **88**, 142109 (2006).